

Research Article

Spatial Heterogeneity in Tropospheric Column Ozone over the Indian Subcontinent: Long-Term Climatology and Possible Association with Natural and Anthropogenic Activities

Gayatri Kalita and Pradip Kumar Bhuyan

Centre for Atmospheric Studies, Dibrugarh University, Dibrugarh 786004, India

Correspondence should be addressed to Pradip Kumar Bhuyan, pkbhuyan@gmail.com

Received 17 August 2011; Revised 3 October 2011; Accepted 4 October 2011

Academic Editor: Harry D. Kambezidis

Copyright © 2011 G. Kalita and P. K. Bhuyan. This is an open access article distributed under the Creative Commons Attribution License, which permits unrestricted use, distribution, and reproduction in any medium, provided the original work is properly cited.

Monthly averaged tropospheric ozone residual (TOR) data from TOMS and OMI during the period 1979–2009 are used to study the spatial distribution of tropospheric column ozone within the landmass of the Indian subcontinent, the Tibetan plateau in the north and the Bay of Bengal in the south. The climatological mean shows seasonal maxima in spring and minima in winter in all the regions. The oceanic regions exhibit broad summer maximum and the maximum to minimum ratio is the lowest for these regions. The concentration of tropospheric column ozone is found to be highest in North Eastern India (NE) and the Indo Gangetic plains (IGP). NE ozone concentration exceeds that of IGP during spring whereas in post monsoon and winter reverse is the case. In the monsoon season, O₃ levels in the two regions are equal. The spring time highest level of tropospheric column ozone over NE region is found to be associated with highest incidence of lightning and biomass burning activity. The Stratosphere-Troposphere exchange is also found to contribute to the enhanced level of ozone in spring in NE India. A net decrease in tropospheric ozone concentration over NE during the period 1979 to 2009 has been observed.

1. Introduction

Tropospheric ozone is a secondary pollutant which is not emitted directly into the atmosphere but is formed in situ from complex mixture of precursor pollutants such as carbon monoxides, volatile organic compounds, and nitrogen oxides (CO, VOC, and NO_x). These precursors are produced both naturally and anthropogenically, where natural sources include the vegetations, forest fires, wetlands, and so forth, and anthropogenic sources are vehicle exhausts, biomass burning, industrial emissions, and so forth. Depending upon the precursor strength, the concentration of tropospheric ozone varies spatially and temporally over the globe. The nonlinear influence of NO_x and VOC emissions on ozone formation and destruction, the influence of transport and dispersion processes on the atmospheric distribution of chemical compounds, and the vast differences in their chemical lifetimes induce diversity.

The ground-based measurements of tropospheric ozone give limited data in time and space, whereas airborne or satellite observations of tropospheric ozone from space offer the opportunity to measure the distribution over large areas, and to study large-scale temporal and spatial behaviour [1, 2]. This is of great importance since ozone formed over source regions, where large amounts of ozone precursors are emitted, can be transported over great distances and affect areas far from the source. Globally, the climatology of tropical tropospheric ozone has been studied in detail in the last two decades from a number of satellite instruments including the total ozone monitoring spectrometer (TOMS) solar backscatter ultraviolet (SBUV) [3, 4] the ozone monitoring instrument (OMI) and microwave limb sounder (MLS) instruments [5–9] and global ozone monitoring experiment (GOME) [10]. Fishman et al. [4] studied the tropospheric ozone burden over the globe using tropospheric ozone residual (TOR) technique and reported the pronounced Northern

Hemispheric pollution feature especially over northeastern India and central China during spring. Further, it is also cited that the tropospheric ozone concentration is relatively less in the Tibetan plateau while south of that region and across the Himalayas in the Ganges River Valley, extending west of Delhi and eastward through Bangladesh and northern Burma, it is much higher. Studies regarding summertime peak suggest that the summertime ozone maxima is a hemispheric-wide phenomenon [4, 11–14]. The quantitative assessment of tropical tropospheric ozone-controlling factors by Sauvage et al. [9] has inferred that lightning is the dominant contributor accounting for more than 28% of the annual average of tropical tropospheric O₃ burden. Other contributions from surface sources are relatively smaller, with nearly 7% for soils and for biomass burning, around 8% for anthropogenic sources on annual average with 1% sensitivity, while the stratosphere-troposphere exchange (STE) accounts for 5% of tropical tropospheric O₃, and the O₃ background accounts for 30% of the tropical tropospheric O₃ burden in the absence of tropical NO_x sources. STE in the tropics and extratropics has always been considered as one of the major source of tropospheric ozone in addition to the photochemically induced heterogeneous chemistry of ozone production though quantification of STE budget remains difficult [15–18].

In the Indian tropical region, with increasing emissions of O₃ precursors such as oxides of nitrogen (NO_x), volatile organic compounds (VOCs) [19], carbon monoxide (CO) [20], and nonmethane hydrocarbons (NMHCs) [21] from traffic, industry and large-scale biomass burning, the potential of tropospheric O₃ production is enhanced [22–26]. The tropospheric ozone production mostly depends on photochemical reactions of the precursors, and thus the long-term trend over the Indian region shows a latitudinal gradient [27]. Another significant study on Indian zone tropospheric ozone [28] reveals the impact of higher anthropogenic pollution associated with economic growth in the post nineties on the enhancement of tropospheric ozone. Studies over Indo Gangetic Plain (IGP) have pointed out repeatedly the effect of anthropogenic emission on the concentration of tropospheric ozone [29, 30].

The aim of the present study is to investigate the spatial diversity of tropospheric ozone column within the Indian subcontinent, the adjoining Tibetan Plateau, and the Bay of Bengal and to identify the mechanisms responsible for high level of tropospheric ozone in the remote nonindustrialized Northeastern region of India as compared to that in the well-known highly polluted Indo Gangetic Plains of North India. The long-term trend in tropospheric column ozone over NE India has also been studied.

2. The Study Area

For systematic investigation of the spatial heterogeneity of tropospheric ozone within the Indian subcontinent, the whole area including the Tibetan plateau and the Bay of Bengal is gridded into seven different regimes, coded as Tibetan Himalayas (TH), Indo Gangetic Plains (IGP), Mainland India (ML), Southern India (SI), Northeast India

(NE), North Bay of Bengal (NBoB), and South Bay of Bengal (SBoB). The regions have been divided taking into consideration the topography, population density and industrial activity as shown in Figure 1. TH covers the northern most region of India including the high Tibetan glaciers. This is a sparsely populated region having almost nil industrial activity. IGP covers the entire Indo Gangetic Plains upto Bay of Bengal. The high population density in the entire belt and heavy industrialization always draws the attention of being one of the highly polluted regions of Northern Hemisphere. The higher emission from industries and transportations over the IGP has been reported and discussed earlier [30–35]. The mainland India (ML) includes the central Indian landmass which is relatively drier and hilly compared to IGP. However, the hills are not so high as in the TH, and also the region is less industrialized than IGP except in the west. North eastern India is separately figured out as NE, because of its peculiar topography of hills and plains covered with evergreen dense forests. Situated at the foothills of the Himalayas, the climate in NE India is different from the rest of the country. The varied physiological features and altitudinal differences of the region give rise to varied types of climate ranging from near tropical to temperate and alpine [36]. SI covers the southern coast of India, near to the equator, largely affected by oceanic activity that leads to humid coastal environment. The NBoB and SBoB are the two regions of Bay of Bengal namely northern Bay of Bengal and southern Bay of Bengal, respectively. The atmospheric concentration of northern BoB has been reported to be modulated by industrial pollution and biomass-burning-emissions carried from various regions in northern India and Bangladesh by synoptic winds, and, hence, average pollution level is higher in northern BoB compared to southern BoB [37]. The importance of the study of these two water regimes lies in its synoptic conditions that influence the climate pattern of the entire subcontinent. Moreover, the existence of intertropical convergence zone (ITCZ) is responsible for convective activity over southern India as well as in northeastern India [38]. The strong cyclonic activity in BoB which supplies moisture along with local convection is favorable for the genesis of thunderstorms over northern India. The cyclonic activity also uplifts particulate matter loading over Northern India [39].

3. Data

3.1. Tropospheric Column Ozone. The tropospheric column ozone (Trop O₃) dataset used for the study includes combined tropospheric ozone residual (TOR) data from 1979 to 2005 determined from version 7 Earth Probe (EP) total ozone monitoring spectrometer (TOMS) and solar backscatter ultraviolet (SBUV) for a given day by subtracting the 5-day running averaged SBUV stratospheric ozone data from the total ozone data at each grid point [4]. The tropospheric column ozone data determined by subtracting measurements of microwave limb sounder (MLS) stratospheric column ozone from ozone monitoring instrument (OMI) measured total column ozone after adjusting the intercalibration differences of the two instruments using the convective cloud differential (CCD) method used during the

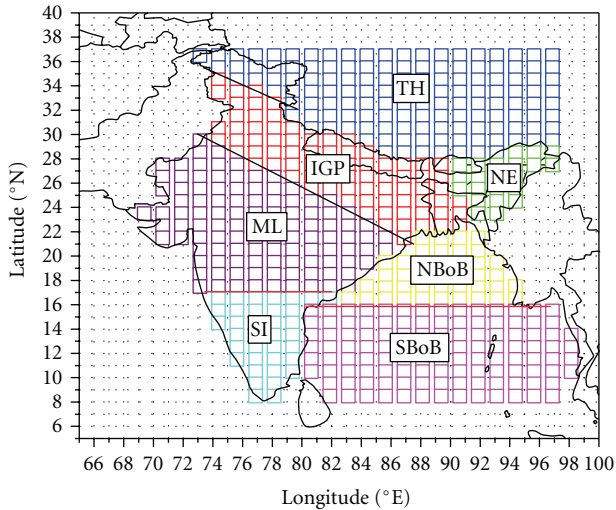


FIGURE 1: Indian landmass, the Tibetan glaciers, and the Bay of Bengal divided into different regions as represented by the area covered by the small square grids of same colour.

period 2006–2009 [6]. The OMI/MLS tropospheric column ozone data is produced using an improved version of the tropospheric ozone residual (TOR) method developed for TOMS [40]. The continuity of TOMS/SBUV TOR data and OMI/MLS tropospheric ozone data is based on the validation of the OMI total ozone measurements with EP/TOMS and SBUV measurements and OMI/MLS tropospheric ozone validation which entail comparisons between MLS SCO and SCO determined from the CCD method [6]. Further details of the TOR and Trop O₃ retrieval informations are given by Fishman et al. [4], Levelt et al. [40], and Ziemke et al. [6]. Kar et al. [30] has recently reported the combined study of TOMS and OMI tropospheric column ozone over the Indo Gangetic Plain. The monthly averaged tropospheric ozone data available at $1^\circ \times 1.25^\circ$ (latitude \times longitude) resolution from January 1979 to December 2009 (http://acd-ext.gsfc.nasa.gov/Data_services/cloud_slice/new_data.html, ftp://jwocky.gsfc.nasa.gov/pub/ccd/data_monthly_new) are utilized. The following supplementary data sets have been used to explain the observed characteristics of Trop O₃.

3.2. Tropospheric NO₂. The monthly mean tropospheric column NO₂ measurements for the period 1996–2009 are analyzed to study the trend and variability over specific regions from the satellite instruments global ozone monitoring experiment (GOME) from March 1996 till December 2002 and Scanning Imaging Absorption SpectroMeter for Atmospheric Cartography (SCIAMACHY) from January 2003 till December 2009. The GOME and SCIAMACHY satellite spectrometers measure backscattered light from the Earth's atmosphere in the UV and visible wavelength range. GOME NO₂ observations are available since 1995 with a global coverage every 3 days. Since July 2003, a technical failure aboard the ERS platform resulted in a strongly reduced coverage. Since 2002, SCIAMACHY is observing the atmosphere in alternating limb and nadir direction. For tropo-

spheric NO₂ retrievals, only the nadir observations are used, resulting in a global coverage every 6 days [41]. Van der et al. [41, 42] has studied the NO_x variability and trend over China and over the globe, respectively, combining the GOME and SCIAMACHY from 1996–2006. The consistent dataset at $0.25^\circ \times 0.25^\circ$ (latitude \times longitude) resolution (<http://www.temis.nl/airpollution/no2.html>) are well validated to avoid the systematic differences in the trend analysis [41, 43].

3.3. Lightning Flash Density. The quality checked monthly lightning activity obtained from lightning imaging sensor (LIS) on board the Tropical Rainfall Measuring Mission (TRMM) satellite of Marshall Space Flight Center for the period of 1998–2009 are used in this study. LIS observes lightning activity over the tropical region bounded by 35°N – 35°S . This instrument detects total lightning, which includes cloud-to-ground, intracloud, and cloud-to-cloud discharges. The LIS is useful for identifying the spatial location of lightning, time of lightning events, and radiant energy from lightning activity. The monthly total lightning flash counts are gridded with a spatial resolution of $0.5^\circ \times 0.5^\circ$.

3.4. Fire Counts. To identify the regions of biomass burning, the fire count data obtained by the moderate resolution imaging spectroradiometer (MODIS) have been used. The gridded MODIS active fire products present statistical summaries of fire pixel information [44]. The products are generated at 1 degree spatial resolution for time period of one calendar month. These products are generated from MODIS CMG 0.5 degree products [44]. The MODIS fire products include four individual data sets within one file: CorrFirePix (overpass corrected fire pixel count), Cloud CorrFirePix (overpass and cloud corrected fire pixel count), Mean Power (mean Fire Radiative Power), and Mean Cloud Fraction (mean Cloud Fraction). Monthly mean fire count data from 2000–2009 obtained from both Terra and Aqua satellites have been used in the present study.

3.5. Air Back Trajectory. To identify the source regions, the air mass back trajectories analysis has been carried out using the hybrid single particle lagrangian integrated trajectory (HYSPLIT) model from NOAA ARL [45], (<http://ready.arl.noaa.gov/HYSPLIT.php>). In addition, vertical wind (VW) data obtained from NCEP/NCAR reanalysis at 6UT (<http://www.cdc.noaa.gov/>) for pressure level 100 hPa were examined on month-to-month basis from January 1979–December 2009. The vertical wind (omega) is the pressure gradient in the units of Pascal/sec, and the positive and negative values in vertical wind represent updraft and down-draft, respectively.

4. Results

4.1. Climatology of Tropospheric Column Ozone. The monthly mean Trop O₃ averaged for the period 1979–2009 grouped into respective zones as described earlier is shown in Figure 2. Generally, Trop O₃ is minimum in winter months and maximum in summer months. However, the magnitude of the

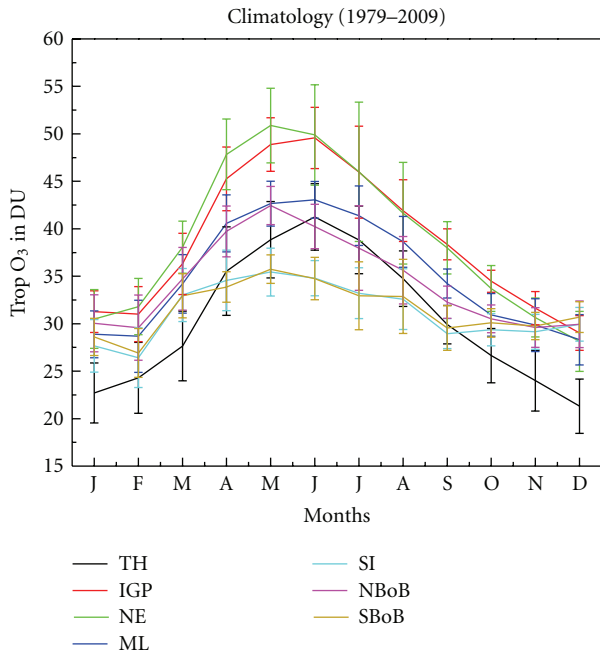


FIGURE 2: Month-to-month variation of tropospheric column ozone measured by TOMS and OMI satellites over TH, NE, IGP, ML, SI, NBoB, and SBoB averaged for the period 1979–2009. The vertical bars represent the standard deviation from the mean.

ozone column burden in the troposphere of each zone varies significantly. Trop O_3 is lowest in Tibetan Himalayas from October to March, while it is lowest in SI and SBoB from April to September. The tropospheric column ozone over TH surpasses that of SI and SBOB in these months of the year. It is also noted that the amount of tropospheric ozone over SI and SBoB is nearly equal all throughout the year. This is possibly due to the fact that SI and SBoB are around the equator, and production and loss mechanism are likely to be influenced by the ocean, where precursors are less for ozone production. The broad summer maximum is often associated with the photochemical production of ozone [46, 47]. The time of occurrence of the annual peak varies from zone to zone. Tropospheric column ozone maximizes in the month of May in NE, NBoB, SI, and SBoB while it peaks in the month of June in IGP, ML, and TH. The summer-to-winter ratio is highest for NE and IGP whereas it is lowest for SI and SBOB. In addition, the level of tropospheric ozone concentration is higher over NE and IGP with sharp seasonal peak, maybe due to higher concentration of pollutants due to anthropogenic activity. The spring time ozone maxima observed in the tropics and in the mid latitudes of Northern Hemisphere are attributed to the natural and anthropogenic emissions enhanced by dynamical phenomena [13, 14, 48].

It is further observed from Figure 2 that the level of tropospheric column ozone concentration is highest over NE during the dry and hotter months of the year, that is, from February to June. But during monsoon, average ozone concentration in both IGP and NE coincides followed by higher concentration over IGP in postmonsoon and winter months.

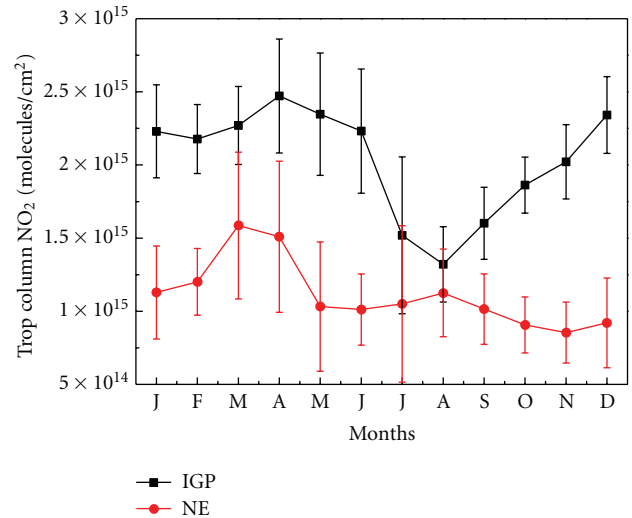


FIGURE 3: Month-to-month variation of tropospheric NO_2 measured by SCIAMACHY and GOME over IGP and NE from 1996–2009.

The annual maximum occurs in May over NE and in June over IGP. Kar et al. 2010 [30], reported higher tropospheric ozone concentration over Eastern IGP than that in the entire IGP belt. The long-term monthly average of tropospheric O_3 during winter to spring months over NE being higher than that over IGP is a significant observation from environment point of view as the NE region is not as densely populated (123 persons per sq. km) and industrialized [49] as the IGP. The IGP is one of the most densely populated areas of the world (456 persons per sq.km) [50] where pollution from different emission processes contribute to air quality degradation. Even though the absolute difference of O_3 concentrations between NE and IGP appears small, in view of the different regional characteristics and also in view of the trend being for last 30 years, it would be worthwhile to thoroughly investigate the observed seasonal trends in terms of sources and sinks in these two regions.

4.2. Role of Precursors. NO_2 is known to be the primary precursor of ozone and greatly involved in balancing the ozone concentration. To examine the cause of higher level of ozone over NE, the monthly average from April 1996–December 2009 NO_2 concentration over the NE and IGP regimes has been compared and shown in Figure 3. The long-term monthly average shows that level of NO_2 over IGP is nearly double than that of NE in most of the months, except in monsoon. Though the NO_2 concentration over NE is not exactly half of IGP during monsoon, still it is lower, and, thereafter, the concentration over IGP increases whereas over NE it decreases. Thus, it is reasonable to believe that NO_2 is not the primary source of tropospheric O_3 over the NE region at least during the first half of the year from February to May. Between the seasons, tropospheric NO_2 is observed to be maximum in spring and minimum in monsoon months. Over IGP, a significant secondary peak is also observed during winter. This may be attributed to

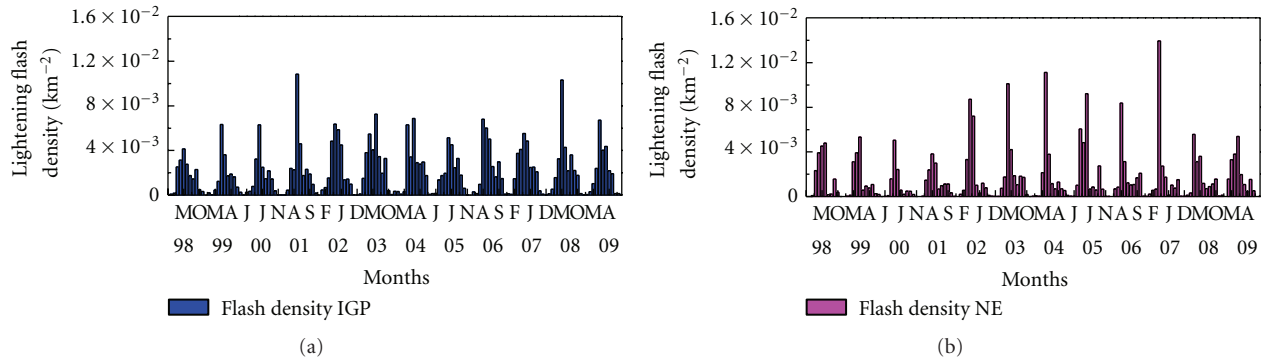


FIGURE 4: Monthly lightning flash density over NE and IGP from 1998–2009 as obtained by the LIS on board TRMM satellite.

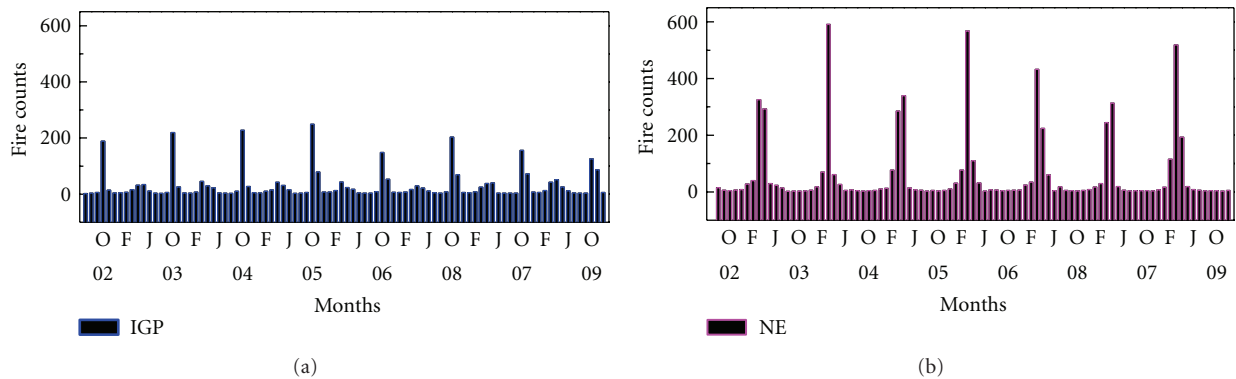


FIGURE 5: MODIS Aqua fire counts averaged for each month from 2002–2009.

the similar source over IGP which explains the finer mode aerosol loading enhancement during winter [51]. In a recent study of tropospheric NO₂ column over India, Prasad et al. [52] have shown that the high mean concentration over IGP is associated with the location of major thermal power plants and population density. The spring time higher concentration of both tropospheric NO₂ and O₃ resembles the higher aerosol loading over NE India in this season [53, 54] which is attributed to transportation across IGP in addition to the local emissions.

The ambient temperature over NE begins to rise from March onwards till summer and moderate rainfall with lightning, and thunderstorm is experienced in April and May. NO_x produced by lightning is a major contributor to the ozone in the upper troposphere and provides the NO₂ that produces the upper tropospheric O₃ [9]. Lightning also can produce O₃ directly by discharge of O₂. Lightning is a massive flow of electrons that superheats gas to a conductive plasma state and radiates broad spectrum energetic radiation, including ionizing radiation. Therefore, oxygen atoms are formed which combine with oxygen molecules to produce ozone. When lightning occurs, about 10% of the atmosphere surrounding it is converted into ozone [55]. In Figure 4 the lightning flash density over IGP and NE is plotted from which it is observed that the lightning activity is seasonal, and, in both IGP and NE, it maximizes in spring or early monsoon (March–June) months. However, it is to be noted

that the lightning activity in NE is more than that in IGP in most of years for which data are available. It may also be noted that the activity peak in NE precedes that of IGP by at least a month. The advanced spring time higher flash density over NE may contribute to the higher level of ozone than IGP in spring months. Earlier it was reported that the lightning activity over the Indian subcontinent is maximum in April/June in the region covering 80°E–100°E within the latitude belt of 25.2°N–26.6°N [38]. Martin et al. [56] reported significant correlation of tropospheric column ozone variability and in phase seasonality upto 20% with the lightning activity. During spring or premonsoon, synoptic conditions over BoB lead to maximum lightning activity, and the anticyclone intensity contributes significantly to the incursion of moisture in different parts of NE India [38].

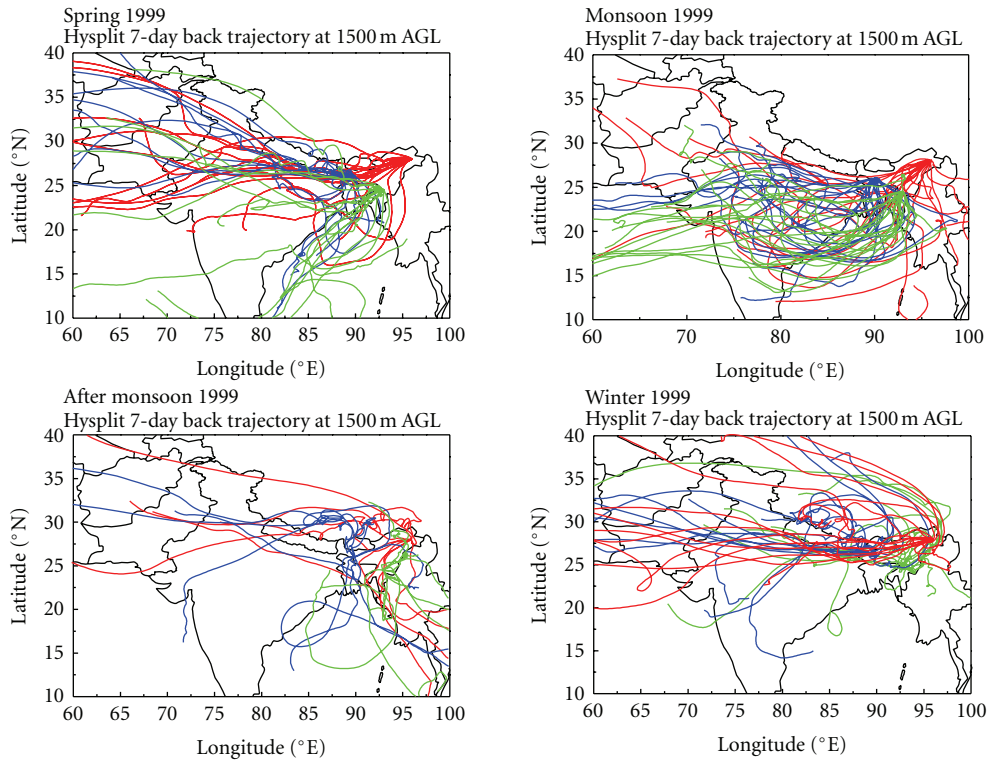
The fire counts are indicative of the natural and anthropogenic biomass burning, where large amounts of CO, CH₄, VOC, and NMHC are emitted besides NO_x. Ozone is formed when CO, CH₄, and NMHC react in the presence of NO_x and sunlight [57]. The ozone production efficiency is observed to be higher in the lower troposphere near to the biomass burning plumes, and there is net increase in the mixing ratios of ozone and its precursors [38]. The long-term (2002–2009) average of fire count from MODIS Terra and Aqua satellites shows higher fire counts over NE than in IGP (Figure 5) in spring which is the post harvesting and relatively dry season for NE. However, in the postmonsoon and winter season,

fire counts are observed to be higher in IGP than in NE. The annual burning activity for NE peaks in spring whereas in IGP it is in postmonsoon. The important point noted is the similarity in the seasonal patterns of fire counts with tropospheric ozone for these two regimes. From February to May over NE region, both tropospheric ozone and fire counts exceed the IGP and, with the end of the dry season both the entities coincide in both regimes, finally in post monsoon and winter, IGP leads the NE. Biomass burning associated with shifting cultivation practices in the north eastern region of India is an important source of trace gas emissions in the Southeast Asian region [58]. Number of studies have cited the effect of natural and anthropogenic fires on the seasonal variation of particulate as well as trace gas loading over IGP and NE India. The anthropogenic fossil fuel and biofuel combustion contribute to the winter time fine mode carbonaceous and sulphate aerosols enhancement in shallow boundary layer with relatively stable atmospheric conditions [51, 59]. However, it is also cited that though the aerosol loading is higher in premonsoon, the particles are basically coarse mode mostly influenced by transportation from northwestern India and West Asia [32, 33, 35, 52]. The forest burning emissions are examined as a potential dominant contributor to the enhancement of the aerosol index in the NE India with highest range during March–May [60]. The similar seasonal pattern between fire counts and tropospheric ozone found in the present study indicates that the higher level of tropospheric column ozone is the direct consequence of biomass burning over the region in respective seasons. The onsite measurement of biomass burning from grassland during spring over NE India [58, 61] reveals the emission of ozone precursors (NO_x , CO, CH₄, NMHC, etc.) in large amounts. The correlation between the columnar tropospheric ozone and biomass burning has already been well documented [26, 62]. The one-to-one correlation of biomass burning with tropospheric ozone variation was reported earlier by Kita et al. [63], de Laat [64], and Kondo et al. [65]. Thus, it can be inferred that the burning activity triggers enhancement of ozone concentration over NE. As in the NE India, South East Asia also experiences intense biomass burning activity in the dry season as reported by van der Werf et al. [66]. Convective activity over South East Asia frequently moved boundary layer air impacted by biomass burning to the free troposphere [65] part of which might eventually reach the NE region of India through transport.

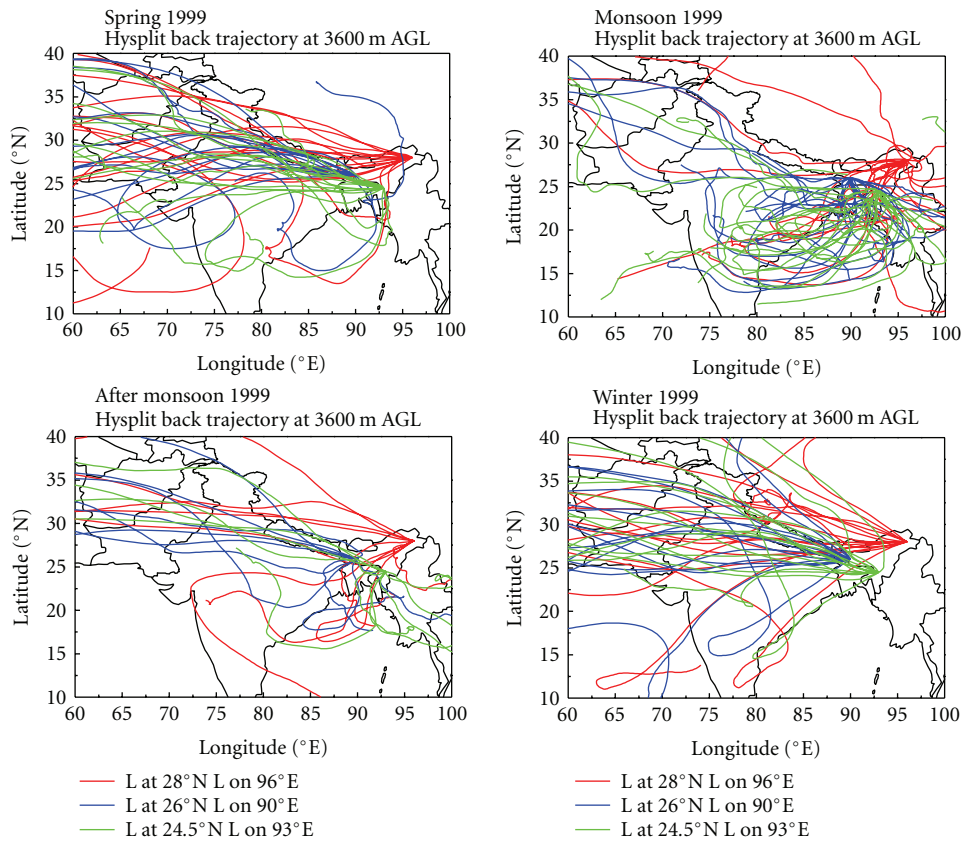
Transportation from IGP to the NE is seen to be another important factor causing higher O₃ level over NE. The transportation of natural as well as strong anthropogenic emissions across IGP and South East Asia enhances the finer mode aerosol loading over eastern BoB [67–69]. The winds originating from northeastern region of Indian subcontinent as well as from southeast Asian countries largely affect the BoB during the late NE-monsoon [70]. To investigate the effect of air mass transportation on enhancement of O₃ concentration, we divided the NE region into three different transport regimes: in extreme northeast corner at 28°N and 96°E, in the south 24.5°N and 93°E, and in west at 26°N and 90°E. While selecting the endpoints of the trajectory high altitude regions are ignored. The 7-day backward trajec-

tory analysis using NOAA HYSPLIT model at 1500 m and 3600 m above ground level at the selected multiple locations of NE region shows that, except monsoon in rest of the three seasons, the trajectories are across the IGP region. The trajectories observed in all the years are almost similar, and representative trajectories for the year 1999 are shown in Figures 6(a) and 6(b) at 1500 m and 3600 m above the ground level. During monsoon, the trajectories pass through the BoB to all the three locations. Hence, the probability of precursor advection to NE from IGP reduces in monsoon compared to the other seasons. Thus, the higher concentration of ozone over NE in spring is due to the combined influence of air-mass transportation from the IGP in addition to the substantial photochemical production from precursors from increased biomass burning and lightning activity in this particular season. In postmonsoon near to the boundary layer, strong south easterly wind prevails through BoB in addition to the trajectories across IGP. While at 3600 m above the ground level, the trajectories are mixed and enter only through the western channel to NE India. In winter months, back trajectories show transportation through IGP and across the Tibetan plateau which is high altitude region. It has been reported earlier by Mauzerall et al. [71] that the seasonal changes in net O₃ production over East Asia is strongly influenced by seasonal changes in transport. Moreover, in the wet season, clean oceanic air from Indian Ocean and BoB brings air low in O₃ and O₃ precursors into the region, while in the dry season ozone concentration greatly increases due to regional biomass burning which is most intense at the end of the dry season [71, 72]. The Frontier Research System for Global Change University of California, Irvine (FRSGUCI) Chemical transport model (CTM) study [73] inferred that, in spring and autumn, efficient vertical transport out of the boundary layer, rapid horizontal transport in the upper troposphere, and significant chemical formation combine to give the greatest ozone enhancements downwind in the East Asia, while in winter vertical transport is limited, and the main export from the boundary layer is southwesterly, towards the Indian subcontinent. The advection of East Asian pollution to north east Asia was reported by Mauzerall et al. [71] using MOZART model hypothesis and by Wild and Akimoto [73] using FRSGUCI chemical transport model. Thus it can be inferred that long-range transportation of air mass is highly seasonal.

Vertical intrusion from the stratosphere is also an important source of tropospheric O₃ in the tropics [13]. The vertical transport is induced by synoptic scale and small-scale meteorological phenomena or induced by topography. The NE zone is in the Himalayan foothills, and as such there is a strong probability of downward transport of ozone. The NCEP vertical wind at 100 m bar corresponding to 15 km height is plotted as shown in Figure 7. It is observed that there is a net positive pressure gradient which signifies the net downward flux. So there is the probability of downward flux from the stratosphere influencing the O₃ tropospheric ozone budget in the NE through vertical exchange. The maximum in the stratosphere to troposphere flux occurs in the mid latitudes of northern hemisphere in late winter/spring [13].



(a)



(b)

FIGURE 6: (a) Seasonal 7-day air back trajectory at 1500 m above ground level (AGL) for the year 1999 at the three different points of NE. (b) Seasonal 7-day air back trajectory at 3600 m above ground level (AGL) for the year 1999 at the three different points of NE.

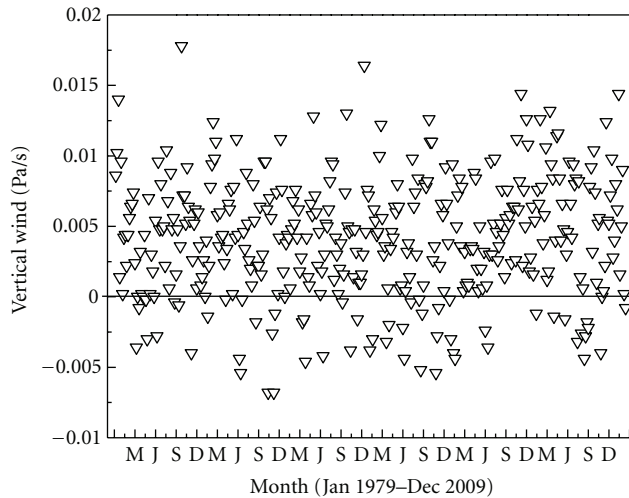


FIGURE 7: NCEP/NCAR reanalysis vertical wind at 100 hpa over NE from 1979–2009.

It is further reported that there is a hemispheric difference in stratospheric tropospheric exchange (STE) which acts as major contributor to summer time maxima and is possibly due to less probability of Rossby wave forcing in the midstratosphere and mesosphere of the SH than NH [13].

4.3. Long-Term Trend in Tropospheric Ozone over NE. Before analyzing the long-term trend of tropospheric column ozone over NE using datasets of Nimbus/TOMS, Earth Probe/TOMS, and OMI, the consistency between the datasets is checked. The intercomparison of tropospheric column ozone data from Earth Probe/TOMS and OMI sensors has been performed for available overlapping period October 2004–December 2005 over NE regions. The results show close agreement between the two measurements as shown in Figure 8 ($R = 0.66$ with confidence exceeding 99%). Unfortunately, the observation of Nimbus/TOMS and EP/TOMS did not overlap for any period, and hence no intercomparison could be performed between these two data sets.

To investigate the long-term trend of tropospheric column ozone over NE, we have normalized the monthly mean tropospheric column ozone by using the following relation:

$$\text{Trop } O_{3\text{norm}} = \text{Trop } O_{3\text{ave}} - \text{Trop } O_{3\text{mon}}, \quad (1)$$

where $\text{Trop } O_{3\text{norm}}$ is the normalized value for a given month, $\text{Trop } O_{3\text{ave}}$ is value averaged over thirty years for the same month, and $\text{Trop } O_{3\text{mon}}$ is the value for the same month.

The tropospheric ozone anomaly (i.e., the normalized ozone being higher or lower than the average) during 1979–2009 shows that it remains mostly positive from 1979 till 1993 (Figure 9(a)), and thereafter it starts decreasing. Critical examination of the data shows that the anomaly starts decreasing after replacement of the satellite TOMS Nimbus with TOMS Earth probe in 1997, while before that (1979–1994) the ozone level remained unchanged (slope = 0.007). The gradual fall continues with OMI too and the level

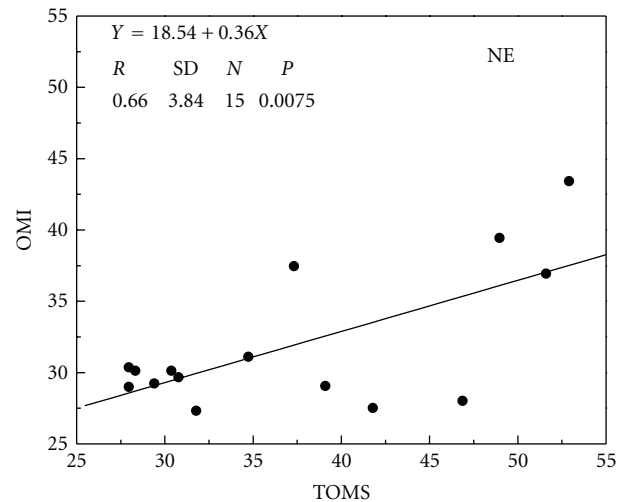
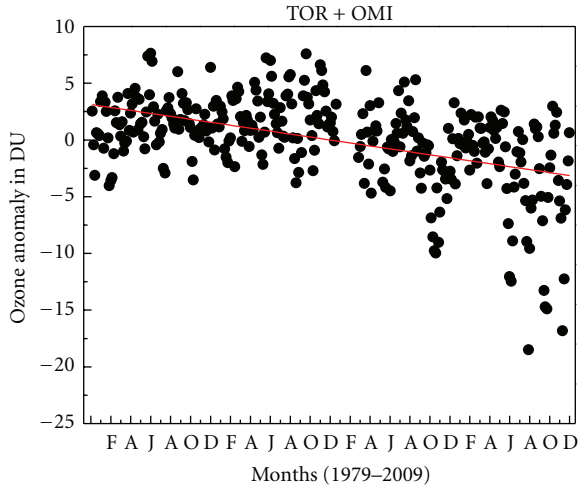


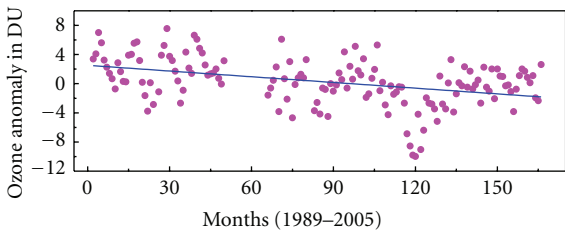
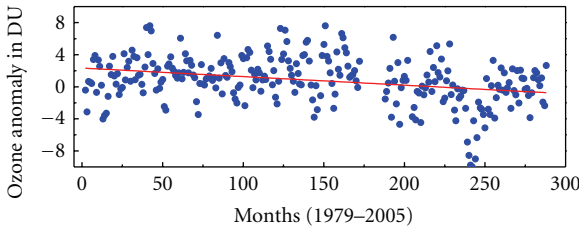
FIGURE 8: Intercomparison of tropospheric ozone over the NE region using data from simultaneous measurement by TOMS and OMI sensors for the period October 2004–December 2005.

decreases faster for OMI-observed O_3 data. To examine whether the downward trend is due to the use of different set of data clubbed together, the data sets are taken separately and the trend studied. From 1979–2009, the regression analysis showed a negative trend with slope -0.01 ($P < 0.001$) (Figure 9(a)) and, from 1979–2005 similar trend continues with negative slope -0.01 ($P < 0.001$) (Figure 9(b)). The decreasing trend in tropospheric ozone over NE is found even while data from a single satellite is used. It is to be noted that the tropospheric ozone burden started to decrease from 1989 onward. A more negative slope of -0.02 ($P \sim 0.001$) is observed during 1989–2005 TOR trend over NE (Figure 9(b)). Although the negative slope during 1997–2005 is negligible, a slight decrease in the trend is observed (Figure 9(c)).

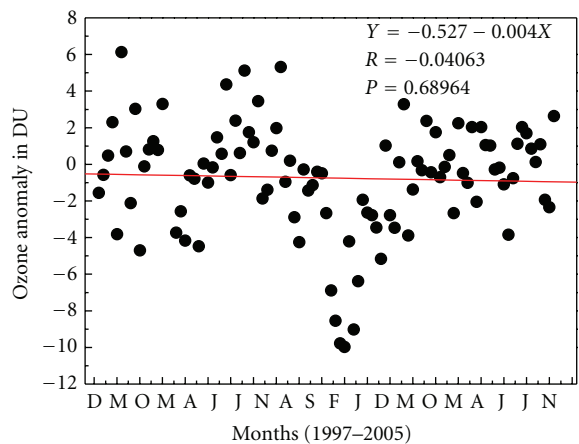
Therefore, it may be concluded that the decrease in tropospheric column O_3 is real while the rate of decrease remains inconclusive. A detailed study of sensors of the satellite is beyond the scope of the present study. However, different studies have already been undertaken using combined satellite ozone dataset. For example, the long-term trend analysis of tropospheric ozone over Indian region by Saraf and Beig [27] has not mentioned any inconsistency between the sensors of satellite instrument for combined study of Nimbus 7/TOMS and Earth Probe/TOMS. The comparison of total column ozone between Earth Probe/TOMS and OMI reported that Earth Probe/TOMS is lower than OMI by about 8–15 DU [74]. The inconsistency in the data set of TOR from TOMS and tropospheric column ozone from OMI earlier reported by Kar et al. [30], where OMI observation shows more localized enhancement rather than along the entire belt of IGP. For comparison of aerosol index from Earth Probe/TOMS and Nimbus 7/TOMS, Hsu et al. [75] and Habib et al. [60] recommended the scale factor of 0.75. While using the Earth Probe/TOMS, Nimbus/TOMS and OMI to study the aerosol index, Gautam et al. [51]



(a)



(b)



(c)

FIGURE 9: (a) Scatter plot of monthly normalized tropospheric ozone over NE for the entire period 1979–2009. The solid line is the linear regression through the points. (b) Scatter plot of normalized monthly tropospheric O₃ over NE as obtained using only TOR data for the period 1979–2005 (top) and 1989–2005 (bottom). (c) Scatter plot of normalized monthly tropospheric O₃ over NE as obtained using TOR data only for the period 1997–2005.

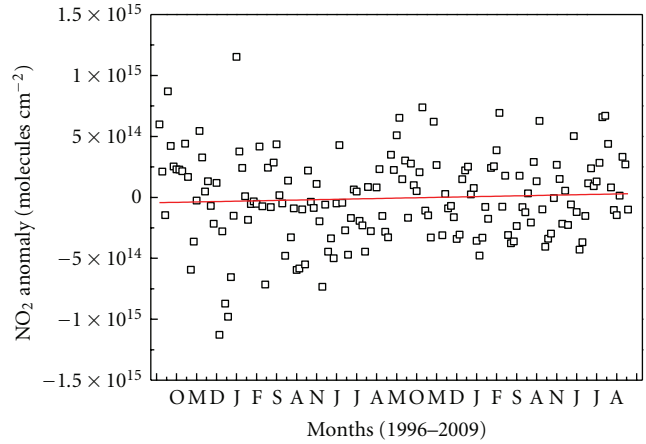


FIGURE 10: Monthly normalized NO₂ over NE plotted for the period April 1996–December 2009.

showed that the earth Probe/TOMS overestimates the OMI observation. However, in the present study as has been shown, the gradual negative trend is seen irrespective of the data sets (i.e., satellite platforms) and, therefore, signifies that the precursors are escaping from the region. The average NO₂ trend over NE was found to be almost same throughout the twelve years (1996–2009) period during which data are available (Figure 10). The average lightning activity over NE, however, has been found to be increasing which in general has maximum contribution to the tropical tropospheric ozone concentration as reported by Sauvage et al. [9].

5. Conclusions

- (i) Long-term climatology of tropospheric column ozone over different parts of the Indian subcontinent and adjoining areas shows maximum in spring and minimum in winter months except for the oceanic regions where a broad summer maximum is observed.
- (ii) The concentration of tropospheric ozone is highest in North Eastern India and Indo Gangetic plains. NE ozone concentration exceeds that of IGP during spring whereas in postmonsoon and winter reverse is the case. In the monsoon season, O₃ levels in the two regions are equal.
- (iii) The spring time highest level of tropospheric column ozone over NE region was found to be associated with highest incidence of lightning activity in this season.
- (iv) Very good correlation between biomass burning activity and tropospheric ozone concentration over NE and IGP has been observed.
- (v) The stratosphere-troposphere exchange also contributes to the enhanced level of ozone in spring in NE India.
- (vi) There has been a net decrease in tropospheric ozone concentration over NE from 1979 to 2009.

Acknowledgments

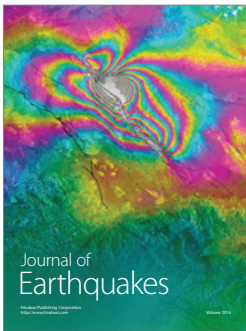
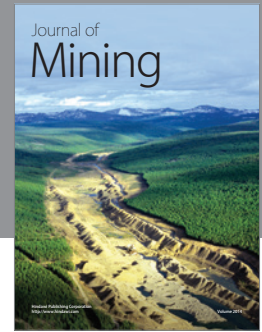
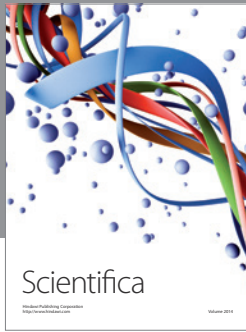
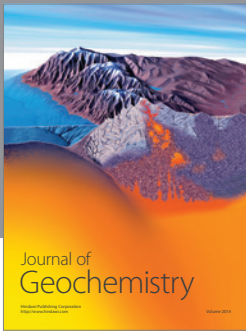
This work is partly financed by the ISRO GBP ATCTM project in which GK is a project fellow. The authors gratefully acknowledge NASA GSFC (<http://acdb-ext.gsfc.nasa.gov/>) for providing the tropospheric ozone data, NASA MSFC (<http://thunder.msfc.nasa.gov/>) for LIS data and GIOVANNI MODIS (<ftp://neespi.gsfc.nasa.gov/data/s4pa/Fire>) for providing fire counts data. The authors also acknowledge the free use of tropospheric NO₂ column data from the YYY sensor from <http://www.temis.nl/>. The authors acknowledge NOAA ARL (<http://ready.arl.noaa.gov/HYSPLIT.php>) for HYSPLIT model and also to NOAA ESRL (<http://www.esrl.noaa.gov/>) for vertical wind data.

References

- [1] K. Y. Kondratyev and C. A. Varotsos, "Remote sensing and global tropospheric ozone observed dynamics," *International Journal of Remote Sensing*, vol. 23, no. 1, pp. 159–178, 2002.
- [2] C. Ahn, J. R. Ziemke, S. Chandra, and P. K. Bhartia, "Derivation of tropospheric column ozone from the Earth Probe TOMS/GOES co-located data sets using the cloud slicing technique," *Journal of Atmospheric and Solar-Terrestrial Physics*, vol. 65, no. 10, pp. 1127–1137, 2003.
- [3] J. Fishman and A. E. Balok, "Calculation of daily tropospheric ozone residuals using TOMS and empirically improved SBUV measurements: application to an ozone pollution episode over the eastern United States," *Journal of Geophysical Research*, vol. 104, no. D23, pp. 30319–30340, 1999.
- [4] J. Fishman, A. E. Wozniak, and J. K. Creilson, "Global distribution of tropospheric ozone from satellite measurements using the empirically corrected tropospheric ozone residual technique: identification of the regional aspects of air pollution," *Atmospheric Chemistry and Physics*, vol. 3, no. 4, pp. 893–907, 2003.
- [5] J. R. Ziemke and S. Chandra, "Seasonal and interannual variabilities in tropical tropospheric ozone," *Journal of Geophysical Research D: Atmospheres*, vol. 104, no. 17, pp. 21425–21442, 1999.
- [6] J. R. Ziemke, S. Chandra, B. N. Duncan et al., "Tropospheric ozone determined from Aura OMI and MLS: evaluation of measurements and comparison with the Global Modeling Initiative's Chemical Transport Model," *Journal of Geophysical Research D: Atmospheres*, vol. 111, no. 19, Article ID D19303, 2006.
- [7] S. Chandra, J. R. Ziemke, P. K. Bhartia, and R. V. Martin, "Tropical tropospheric ozone: implications for dynamics and biomass burning," *Journal of Geophysical Research D: Atmospheres*, vol. 107, no. 14, pp. 1–17, 2002.
- [8] S. Chandra, J. R. Ziemke, and R. V. Martin, "Tropospheric ozone at tropical and middle latitudes derived from TOMS/MLS residual: comparison with a global model," *Journal of Geophysical Research*, vol. 108, no. D9, pp. 4291–4319, 2003.
- [9] B. Sauvage, R. V. Martin, A. van Donkelaar, and J. R. Ziemke, "Quantification of the factors controlling tropical tropospheric ozone and the South Atlantic maximum," *Journal of Geophysical Research D: Atmospheres*, vol. 112, no. 11, Article ID D11309, 2007.
- [10] A. T. J. de Laat, R. J. van der A, and M. van Weele, "Evaluation of tropospheric ozone columns derived from assimilated GOME ozone profile observations," *Atmospheric Chemistry and Physics*, vol. 9, no. 20, pp. 8105–8120, 2009.
- [11] A. Volz and D. Kley, "Evaluation of the Montsouris series of ozone measurements made in the nineteenth century," *Nature*, vol. 332, no. 6161, pp. 240–242, 1988.
- [12] C. Cartalis and C. Varotsos, "Surface ozone in Athens, Greece, at the beginning and at the end of the twentieth century," *Atmospheric Environment*, vol. 28, no. 1, pp. 3–8, 1994.
- [13] P. S. Monks, "A review of the observations and origins of the spring ozone maximum," *Atmospheric Environment*, vol. 34, no. 21, pp. 3545–3561, 2000.
- [14] P. Jing, D. Cunnold, Y. Choi, and Y. Wang, "Summer time tropospheric ozone columns from Aura OMI/MLS measurements versus regional model results over the United States," *Geophysical Research Letters*, vol. 33, p. L17817, 2006.
- [15] C. E. Junge, "Global ozone budget and exchange between stratosphere and troposphere," *Tellus*, vol. 14, pp. 363–377, 1962.
- [16] P. J. Crutzen, "A discussion of the chemistry of some minor constituents in the stratosphere and troposphere," *Pure and Applied Geophysics*, vol. 106–108, no. 1, pp. 1385–1399, 1973.
- [17] W. L. Chameides and J. C. G. Walker, "A photochemical theory for tropospheric ozone," *Journal of Geophysical Research*, vol. 78, pp. 8751–8760, 1973.
- [18] A. Volz-Thomas, "Tropospheric ozone and its control," in *Towards Cleaner Air for Europe—Science, Tools and Applications*, P. Midgley and M. Reuther, Eds., chapter 3, Margraf Publishers, Weikersheim, Germany, 2003.
- [19] L. G. Ivan and C. J. Sollars, "Ambient air levels of volatile organic compounds in Latin American and Asian cities," *Chemosphere*, vol. 36, no. 11, pp. 2497–2506, 1998.
- [20] M. Dalvi, G. Beig, U. Patil, A. Kaginalkar, C. Sharma, and A. P. Mitra, "A GIS based methodology for gridding of large-scale emission inventories: application to carbon-monoxide emissions over Indian region," *Atmospheric Environment*, vol. 40, no. 16, pp. 2995–3007, 2006.
- [21] S. Saito, I. Nagao, and H. Tanaka, "Relationship of NO_x and NMHC to photochemical O₃ production in a coastal and metropolitan areas of Japan," *Atmospheric Environment*, vol. 36, no. 8, pp. 1277–1286, 2002.
- [22] V. Ramanathan, R. J. Cicerone, H. B. Singh, and J. T. Kiehl, "Trace gas trends and their potential role in climate change," *Journal of Geophysical Research*, vol. 90, no. 3, pp. 5547–5566, 1985.
- [23] S. D. Ghude, G. Beig, and S. Polade, "Tropospheric ozone and precursor gases over Indian subcontinent observed from the space," in *Proceedings of the International Symposium on Aerosol-Chemistry-Climate Interaction*, pp. 205–206, Physical Research Laboratory, Ahmedabad, India, November 2007.
- [24] S. D. Ghude, S. Singh, P. S. Kulkarni et al., "Observations and model calculations of direct solar UV irradiances in the Schirmacher region of east Antarctica," *International Journal of Remote Sensing*, vol. 29, no. 20, pp. 5907–5921, 2008.
- [25] G. Beig, S. D. Ghude, S. D. Polade, and B. Tyagi, "Threshold exceedances and cumulative ozone exposure indices at tropical suburban site," *Geophysical Research Letters*, vol. 35, no. 2, Article ID L02802, 2008.
- [26] K. V. S. Badarinath, S. K. Kharol, V. Krishna Prasad et al., "Influence of natural and anthropogenic activities on UV Index variations—a study over tropical urban region using ground based observations and satellite data," *Journal of Atmospheric Chemistry*, vol. 59, no. 3, pp. 219–236, 2008.
- [27] N. Saraf and G. Beig, "Long-term trends in tropospheric ozone over the Indian tropical region," *Geophysical Research Letters*, vol. 31, no. 5, Article ID L05101, 2004.
- [28] P. S. Kulkarni, S. D. Ghude, and D. Bortoli, "Tropospheric ozone (TOR) trend over three major inland Indian cities:

- Delhi, Hyderabad and Bangalore,” *Annales Geophysicae*, vol. 28, no. 10, pp. 1879–1885, 2010.
- [29] P. S. Kulkarni, S. L. Jain, S. D. Ghude, B. C. Arya, P. K. Dubey, and Shah Nawaz, “On some aspects of tropospheric ozone variability over the Indo-Gangetic (IG) basin, India,” *International Journal of Remote Sensing*, vol. 30, no. 15–16, pp. 4111–4122, 2009.
- [30] J. Kar, M. N. Deeter, J. Fishman et al., “Wintertime pollution over the Eastern Indo-Gangetic Plains as observed from MOPITT, CALIPSO and tropospheric ozone residual data,” *Atmospheric Chemistry and Physics*, vol. 10, no. 24, pp. 12273–12283, 2010.
- [31] A. K. Prasad, R. P. Singh, and M. Kafatos, “Influence of coal based thermal power plants on aerosol optical properties in the Indo-Gangetic basin,” *Geophysical Research Letters*, vol. 33, no. 5, Article ID L05805, 2006.
- [32] M. Aloysius, M. Mohan, K. Parameswaran, S. K. George, and P. R. Nair, “Aerosol transport over the Gangetic basin during ISRO-GBP land campaign-II,” *Annales Geophysicae*, vol. 26, no. 3, pp. 431–440, 2008.
- [33] R. Gautam, N. C. Hsu, S. C. Tsay et al., “Accumulation of aerosols over the Indo-Gangetic plains and southern slopes of the Himalayas: distribution, properties and radiative effects during the 2009 pre-monsoon Season,” *Atmospheric Chemistry and Physics Discussions*, vol. 11, no. 5, pp. 15697–15743, 2011.
- [34] D. G. Kaskaoutis, S. K. Kharol, P. R. Sinha et al., “Extremely large anthropogenic aerosol component over the Bay of Bengal during winter season,” *Atmospheric Chemistry and Physics Discussions*, vol. 11, no. 3, pp. 7851–7907, 2011.
- [35] A. K. Srivastava, S. Tiwari, P. C. S. Devara et al., “Pre-monsoon aerosol characteristics over the Indo-Gangetic Basin: implications to climatic impact,” *Annales Geophysicae*, vol. 29, no. 5, pp. 789–804, 2011.
- [36] A. Das, P. K. Ghosh, B. U. Choudhury et al., “Climate change in Northeast India: recent facts and events and worry for agricultural management,” in *Proceedings of the Workshop on Impact of Climate Change on Agriculture*, 2009, ISPRS Archives XXXVIII-8/W3.
- [37] S. K. Satheesh, V. Vinoj, and K. Krishnamoorthy, “Assessment of aerosol radiative impact over oceanic regions adjacent to Indian subcontinent using multi-satellite analysis,” *Advances in Meteorology*, vol. 2010, Article ID 139186, 13 pages, 2010.
- [38] M. R. Ranalkar and H. S. Chaudhari, “Seasonal variation of lightning activity over the Indian subcontinent,” *Meteorology and Atmospheric Physics*, vol. 104, no. 1–2, pp. 125–134, 2009.
- [39] K. V. S. Badarinath, S. K. Kharol, V. Krishna Prasad, D. G. Kaskaoutis, and H. D. Kambezidis, “Variation in aerosol properties over Hyderabad, India during intense cyclonic conditions,” *International Journal of Remote Sensing*, vol. 29, no. 15, pp. 4575–4597, 2008.
- [40] P. F. Levelt, E. Hilsenrath, G. W. Leppelmeier et al., “Science objectives of the ozone monitoring instrument,” *IEEE Transactions on Geoscience and Remote Sensing*, vol. 44, no. 5, pp. 1199–1207, 2006.
- [41] R. J. van der A, D. H. M. U. Peters, H. Eskes et al., “Detection of the trend and seasonal variation in tropospheric NO₂ over China,” *Journal of Geophysical Research*, vol. 111, no. 12, article D12317, 2006.
- [42] R. J. van der A, H. J. Eskes, K. F. Boersma et al., “Trends, seasonal variability and dominant NO_x source derived from a ten year record of NO₂ measured from space,” *Journal of Geophysical Research D: Atmospheres*, vol. 113, no. 4, Article ID D04302, 2008.
- [43] A. Richter, J. P. Burrows, H. Nüß, C. Granier, and U. Niemeier, “Increase in tropospheric nitrogen dioxide over China observed from space,” *Nature*, vol. 437, no. 7055, pp. 129–132, 2005.
- [44] L. Giglio, J. Descloitres, C. O. Justice, and Y. J. Kaufman, “An enhanced contextual fire detection algorithm for MODIS,” *Remote Sensing of Environment*, vol. 87, no. 2–3, pp. 273–282, 2003.
- [45] R. R. Draxler, “Evaluation of an ensemble dispersion calculation,” *Journal of Applied Meteorology*, vol. 42, no. 2, pp. 308–317, 2003.
- [46] A. S. Lefohn, D. S. Shadwick, U. Feister, and V. A. Mohnen, “Surface-level ozone: climate change and evidence for trends,” *Journal of the Air and Waste Management Association*, vol. 42, no. 2, pp. 136–144, 1992.
- [47] R. G. Derwent and T. J. Davies, “Modelling the impact of NO_x or hydrocarbon control on photochemical ozone in Europe,” *Atmospheric Environment*, vol. 28, no. 12, pp. 2039–2052, 1994.
- [48] Y. Choi, Y. Wang, Q. Yang et al., “Spring to summer northward migration of high O₃ over the western North Atlantic,” *Geophysical Research Letters*, vol. 35, no. 4, Article ID L04818, 2008.
- [49] B. Mishra, “Population dynamics, environment and quality of life in North-East India,” in *Proceedings of the Papers of the International Seminar on South-East Asia’s Population in a Changing Asian Context*, 2002.
- [50] <http://envfor.nic.in/unccd/chap-3.pdf>.
- [51] R. Gautam, N. C. Hsu, S. C. Tsay, K. -M. Lau, and M. Kafatos, “Aerosol and rainfall variability over the Indian monsoon region: distributions, trends and coupling,” *Annales Geophysicae*, vol. 27, no. 9, pp. 3691–3703, 2009.
- [52] A. K. Prasad, R. P. Singh, and M. Kafatos, “Influence of coal-based thermal power plants on the spatial-temporal variability of tropospheric NO₂ column over India,” *Environmental Monitoring and Assessment*. In press.
- [53] M. M. Gogoi, K. K. Moorthy, S. S. Babu, and P. K. Bhuyan, “Climatology of columnar aerosol properties and the influence of synoptic conditions: first-time results from the northeastern region of India,” *Journal of Geophysical Research D: Atmospheres*, vol. 114, no. 8, Article ID D08202, 2009.
- [54] B. Pathak, G. Kalita, K. Bhuyan, P. K. Bhuyan, and K. K. Moorthy, “Aerosol temporal characteristics and its impact on shortwave radiative forcing at a location in the North East of India,” *Journal of Geophysical Research*, vol. 115, article D19204, 14 pages, 2010.
- [55] J. R. Sanghvi, “Ozone layer formation through Corona Discharge utilizing natural phenomena,” *International Journal of Energy and Environment*, vol. 2, no. 1, pp. 16–24, 2008.
- [56] R. V. Martin, B. Sauvage, I. Folkins et al., “Space-based constraints on the production of nitric oxide by lightning,” *Journal of Geophysical Research*, vol. 112, no. 9, article D09309, 2007.
- [57] C. S. Atherton, “Biomass burning sources of nitrogen oxides, carbon monoxide and non methane hydrocarbons,” Tech. Rep., DOE Scientific and Technical Information, 1995.
- [58] V. Krishna Prasad, M. Lata, and K. V. S. Badarinath, “Trace gas emissions from biomass burning from northeast region in India Estimates from satellite remote sensing data and GIS,” *Environmentalist*, vol. 23, no. 3, pp. 229–236, 2003.
- [59] R. Gautam, N. C. Hsu, M. Kafatos, and S.-C. Tsay, “Influences of winter haze on fog/low cloud over the Indo-Gangetic plains,” *Journal of Geophysical Research*, vol. 112, article D05207, 2007.
- [60] G. Habib, C. Venkataraman, I. Chiapello, S. Ramachandran, O. Boucher, and M. S. Reddy, “Seasonal and interannual variability in absorbing aerosols over India derived from TOMS:

- relationship to regional meteorology and emissions,” *Atmospheric Environment*, vol. 40, no. 11, pp. 1909–1921, 2006.
- [61] K. V. S. Badarinath, T. R. Kiran Chand, and V. Krishna Prasad, “Emissions from grassland burning in Kaziranga National Park, India—analysis from IRS-P6 AWiFS satellite remote sensing datasets,” *Geocarto International*, vol. 24, no. 2, pp. 89–97, 2009.
- [62] G. Pace, D. Meloni, and A. di Sarra, “Forest fire aerosol over the Mediterranean basin during summer 2003,” *Journal of Geophysical Research D: Atmospheres*, vol. 110, no. 21, Article ID D21202, pp. 1–11, 2005.
- [63] K. Kita, M. Fujiwara, and T. Ogawa, “Biomass burning in the tropics and tropospheric ozone,” *Global Environmental Resources*, vol. 2, pp. 29–37, 1998.
- [64] A. T. J. de Laat, “On the origin of tropospheric O₃ over the Indian Ocean during the winter monsoon: African biomass burning vs. stratosphere-troposphere exchange,” *Atmospheric Chemistry and Physics*, vol. 2, no. 5, pp. 325–341, 2002.
- [65] Y. Kondo, Y. Morino, N. Takegawa et al., “Impacts of biomass burning in Southeast Asia on ozone and reactive nitrogen over the western Pacific in spring,” *Journal of Geophysical Research D: Atmospheres*, vol. 109, no. 15, article D15S12, 2004.
- [66] G. R. van der Werf, J. T. Randerson, L. Giglio, G. J. Collatz, P. S. Kasibhatla, and A. F. Arellano Jr., “Interannual variability in global biomass burning emissions from 1997 to 2004,” *Atmospheric Chemistry and Physics*, vol. 6, no. 11, pp. 3423–3441, 2006.
- [67] V. Ramanathan, P. J. Crutzen, J. T. Kiehl, and D. Rosenfeld, “Aerosols, climate, and the hydrological cycle,” *Science*, vol. 294, no. 5549, pp. 2119–2124, 2001.
- [68] D. Ganguly, A. Jayaraman, and H. Gadhavi, “In situ ship cruise measurements of mass concentration and size distribution of aerosols over Bay of Bengal and their radiative impacts,” *Journal of Geophysical Research*, vol. 110, article D06205, 2005.
- [69] S. K. Kharol, K. V. S. Badarinath, D. G. Kaskaoutis, A. R. Sharma, and B. Gharai, “Influence of continental advection on aerosol characteristics over Bay of Bengal (BoB) in winter: results from W-ICARB cruise experiment,” *Annales Geophysicae*, vol. 29, no. 8, pp. 1423–1438, 2011.
- [70] B. Srinivas, A. Kumar, M. M. Sarin, and A. K. Sudheer, “Impact of continental outflow on chemistry of atmospheric aerosols over tropical Bay of Bengal,” *Atmospheric Chemistry and Physics Discussions*, vol. 11, no. 7, pp. 20667–20712, 2011.
- [71] D. L. Mauzerall, D. Narita, H. Akimoto et al., “Seasonal characteristics of tropospheric ozone production and mixing ratios over East Asia: a global three-dimensional chemical transport model analysis,” *Journal of Geophysical Research D: Atmospheres*, vol. 105, no. 14, pp. 17895–17910, 2000.
- [72] W. M. Hao and M.-H. Liu, “Spatial and temporal distribution of tropical biomass burning,” *Global Biogeochemical Cycles*, vol. 8, no. 4, pp. 495–503, 1994.
- [73] O. Wild and H. Akimoto, “Intercontinental transport and chemical transformation of Ozone and Its Precursors from East Asia,” in *Present and Future of Modeling Global Environmental Change*, T. Matsuno and H. Kida, Eds., pp. 375–382, TERRAPUB, 2001.
- [74] C. Ahn, G. J. Labow et al., “An Initial Comparison of Ozone Monitoring Instrument (OMI) Total Ozone with EP/TOMS, SBUV/2, and Ground Stations,” http://aura.gsfc.nasa.gov/science/publications/OMI-Ahn_Compare_Total_Ozone.pdf.
- [75] N. C. Hsu, J. R. Herman, O. Torres et al., “Comparisons of the TOMS aerosol index with Sun-photometer aerosol optical thickness: results and applications,” *Journal of Geophysical Research D: Atmospheres*, vol. 104, no. 6, pp. 6269–6279, 1999.



Hindawi

Submit your manuscripts at
<http://www.hindawi.com>

